Journal of the European Ceramic Society **16** (1996) 1027–1034
© 1996 Elsevier Science Limited
Printed in Great Britain. All rights reserved
S0955-2219(96)00011-8
0955-2219/96/$15.00

On the Contribution of Notches to the Failure Probability of Ceramic Components

Angelika Brückner-Foit, Armin Heger & Dietrich Munz

Institute of Reliability and Failure Analysis, Karlsruhe University, D-76021 Karlsruhe, Germany

(Received 21 July 1994; revised version received 18 December 1995; accepted 5 January 1996)

Abstract

The failure probability of tensile bars containing circular notches is calculated using the multiaxial Weibull theory. The influence exerted by the stress concentration factor, the stress gradient in the notch root, and the Weibull exponent are analysed. A local risk of rupture is defined, and it is shown how characteristic sub-volumes of the notched tensile bar contribute to the failure probability. An analytical expression is derived which is based on a linear approximation of the stress field in the vicinity of the notch root, and which yields the dependence of the leading term of the failure probability on characteristic quantities such as the stress concentration factor and the Weibull modulus. © 1996 Elsevier Science Limited.

1 Introduction

The design of ceramic components aims at meeting a specific level of reliability instead of specifying a minimum allowable strength due to the inherent scatter of strength. As failure is triggered by the most dangerous flaw, which may be located in a region of comparatively low stress, any stressed volume in the component contributes to the risk of rupture. Hence, the stress distribution of the entire component has to be calculated for design purposes.

This is obviously different from common design practice for metallic components, for which the maximum stress at the most critical point is compared to the strength. Frequently this maximum stress can be determined even if a full stress analysis of the component under consideration has not been made. A well-known example is provided by notches for which analytical and approximate values of the stress concentration factor in the notch root have been determined for a large number of notch geometries.[1,2]

The aim of this study is to investigate the influence of notches on the reliability of ceramic components in order to provide a database from which appropriate design rules can be derived. A well-established theory,[3–6] the so-called multiaxial Weibull theory, is now available, by which the reliability of a ceramic component subjected to an arbitrary stress state can be evaluated. Within the framework of this theory, the reliability is determined via an integral over the stress field. In general, a finite-element analysis of the component under consideration has to be performed prior to the reliability analysis in order to determine the complete stress field with sufficient accuracy. This implies that comparing alternative designs is an arduous task, since a comprehensive finite element analysis is required even for minor modifications of the original design.

It is desirable to assess the contribution of characteristic details such as notches on the basis of tabulated values or preferably on the basis of approximate analytical solutions. For this purpose, simple tensile bars containing notches of various geometries are analysed in this paper using the finite-element method to determine the stress field and using the multiaxial Weibull theory. The dependence of the reliability on the stress concentration factor, on the stress gradient in the notch root and on the material parameters of the ceramic material is determined. An approximate formula for the stress field of a certain class of notches is given from which the contribution of circular notch in a tensile stress field to the risk of rupture can be derived.

2 Weibull Theory for Multiaxial Loading

The failure behaviour of ceramic components subjected to a multiaxial stress state can be assessed using the multiaxial Weibull theory as developed by Batdorf *et al.*[3,4] Evans,[5] and Matsuo.[6] It is assumed that failure is caused by unstable extension of natural flaws of random size, of random location and of random orientation with respect to the principal stress axes. The worst flaw, i.e. the flaw for which the most unfavourable combination

of size, location and orientation is obtained, will propagate unstably and will cause catastrophic failure.

The probability that the size a of a given flaw exceeds the critical crack size a_c is given by:

$$Q_1 = \int_V f_{\mathbf{x}}(\mathbf{x}) \int_\Omega f_{\phi,\theta}(\phi, \theta) \int_{a_c(\mathbf{x},\phi,\theta)}^{\infty} f_a(a)\, da\, d\Omega\, d\mathbf{x} \quad (1)$$

where V denotes the volume of the component considered, Ω the surface of a unit sphere with the polar angles ϕ and θ and surface element $d\Omega = \sin\theta\, d\theta\, d\phi$, $\mathbf{x}$ the coordinate vector, and $f_{\mathbf{x}}(\mathbf{x})$, $f_{\phi,\theta}(\phi,\theta)$, $f_c(a)$ are the probability density functions of the corresponding random variables.

The critical crack size can be determined using fracture mechanics, if the natural flaws can be approximated by planar cracks. Within the framework of this model, a multiaxial stress state gives rise to mixed mode loading of a crack, and the critical crack size is a function of the mode I–III stress intensity factors K_I, K_{II}, K_{III}:

$$a_c = a_c(K_I, K_{II}, K_{III}) \quad (2)$$

with

$$\begin{aligned} K_I &= \sigma_n \sqrt{a}\cdot Y_I \\ K_{II} &= \tau \sqrt{a}\cdot Y_{II} \\ K_{III} &= \tau \sqrt{a}\cdot Y_{III}. \end{aligned} \quad (3)$$

The correction factors Y_I, Y_{II} and Y_{III} represent the influence of the crack geometry. The stress σ_n normal to the crack plane is given by the following relation:

$$\sigma_n = (\sigma_1 \cos^2\phi + \sigma_2 \sin^2\phi)\cdot\sin^2\theta + \sigma_3\cos^2\theta \quad (4)$$

where σ_1, σ_2, and σ_3 are the principal stresses and ϕ and θ are the polar angles determining the orientation of the crack plane relative to the principal axes. The shear stress τ in the crack plane is given by

$$\tau = \sqrt{\tau_{r\phi}^2 + \tau_{r\theta}^2} \quad (5)$$

with

$$\tau_{r\phi} = (\sigma_2 - \sigma_1)\cdot\sin\phi\, \cos\phi\, \sin\theta. \quad (6)$$

and

$$\tau_{r\theta} = (\sigma_1 \cos^2\phi + \sigma_2 \sin^2\phi - \sigma_3)\cdot\sin\theta\, \cos\theta. \quad (7)$$

An equivalent mode I stress intensity factor K_{leq} can be introduced with

$$K_{leq} = \sigma_{eq}\cdot\sqrt{a}\cdot Y_I \quad (8)$$

where the equivalent stress σ_{eq} depends on σ_n, τ and on Y_I, Y_{II}, and Y_{III}. The critical crack size is then given by:

$$a_c = \left(\frac{K_{Ic}}{\sigma_{eq}\cdot Y_I}\right)^2 \quad (9)$$

where K_{Ic} denotes the fracture toughness.

A variety of multiaxiality criteria are given in the literature leading to different expressions for σ_{eq}. A summary can be found in ref 7. An example of one of these criteria is:[8]

$$\sigma_{eq} = \sqrt{\sigma_n^2 + \left(\frac{2}{2-\nu}\right)^2\cdot\tau^2} \quad (10)$$

which is derived using the assumption that the value of the energy release rate in the crack plane determines the onset of unstable crack propagation, and a penny-shaped crack is a suitable model for the natural flaws.

In Weibull theory the following expression is used for the integral over the crack size in eqn (1):[7]

$$\int_{a_c(\mathbf{x},\phi,\theta)}^{\infty} f_a(a)\, da = \left(\frac{\sigma_{eq}(\mathbf{x},\phi,\theta)}{\tau_0}\right)^m \quad (11)$$

where eqn (9) was used for the critical crack size. The parameters m, τ_0 in eqn (11) depend on the toughness of the matrix material and on the statistical properties of the flaw size distribution.

If all locations of flaws and all orientations occur with equal probability, the material is homogeneous and isotropic, and $f_{\mathbf{x}}(\mathbf{x})$ and $f_{\phi,\theta}(\phi,\theta)$ can be replaced by uniform distributions. Hence, Q_1 in eqn (1) is equal to:

$$Q_1 = \frac{1}{V}\int_V \frac{1}{4\pi}\int_\Omega \left(\frac{\sigma_{eq}}{\tau_0}\right)^m d\Omega\, d\mathbf{x}. \quad (12)$$

The number n of cracks in the volume V is also a random variable and can be described by Poisson's distribution. The probability of having exactly n cracks in V is given by:

$$p_n = \frac{M^n\cdot e^{-M}}{n!}, \quad (13)$$

where M is the average number of cracks in V. The following relation for the failure probability P_f is obtained from eqns (12) and (13):[7]

$$P_f = 1 - \exp(-M\cdot Q_1). \quad (14)$$

With the definition of a new material parameter σ_0:

$$\sigma_0 = \tau_0\cdot\left(\frac{V}{V_0\cdot M}\right)^{\frac{1}{m}} \quad (15)$$

where V_0 is a reference or unit volume, the following relation is finally obtained for the failure probability:

$$P_f = 1 - \exp\left(-\frac{1}{V_0}\int_V \frac{1}{4\pi}\int_\Omega \left(\frac{\sigma_{eq}}{\sigma_0}\right)^m d\Omega\, d\mathbf{x}\right). \quad (16)$$

Equation (16) can be rewritten as:

$$P_f = 1 - \exp\left(\left(\frac{\sigma^*}{b}\right)^m\right) \quad (17)$$

where σ^* is a reference stress characterising the loading of the component, and

$$b = \frac{\sigma_0}{H} \tag{18}$$

with the normalised stress integral

$$H = \left(\frac{1}{V_0}\int_V \frac{1}{4\pi}\int_\Omega \left(\frac{\sigma_{eq}}{\sigma^*}\right)^m d\Omega\, dx\right)^{\frac{1}{m}}. \tag{19}$$

Equation (17) implies that the stress at fracture is a Weibull distributed random variable.

The normalised stress integral H is independent of the applied load level and is hence a convenient tool to characterise the effect of the spatial stress distribution on the failure probability, particularly if two components with different geometries are compared. In this case the corresponding Weibull parameters $b^{(1)}$, $b^{(2)}$ (eqn (17)) are related by:

$$\frac{b^{(1)}}{b^{(2)}} = \frac{H^{(2)}}{H^{(1)}}. \tag{20}$$

The allowable stress levels $\sigma^{*(1)}$, $\sigma^{*(2)}$ for two different designs of a component are related by:

$$\frac{\sigma^{(1)*}}{\sigma^{(2)*}} = \frac{H^{(2)}}{H^{(1)}} \tag{21}$$

at a given level of reliability which is characterised by a specific value of P_f. From eqns (17)–(21) it is clear that the information needed for the design of ceramic components is contained in the normalised stress integral, which will be used in the subsequent investigations. However, it should be kept in mind that the numerical value of H depends on the choice of the normalisation volume V_0. The same applies to the ratio of H-values, if the Weibull exponent m is not kept constant.

3 Numerical Evaluation of the Failure Probability

The five-dimensional integral eqn (19) has to be evaluated in order to determine the failure probability or the normalized stress integral H. Conventional numerical integration procedures such as the Gauss integration can be used to integrate over the orientation angles, whereas the integration over the volume is more difficult.

The stress tensor for real structures is generally determined by a finite element analysis, which yields the values of σ_{ij} at a limited number of points within each element, the so-called Gauss points. Because of the high value of m which is obtained for advanced ceramic materials, the gradients of the integrand within each element are very steep, and a large number of evaluation points are needed in order to achieve convergence of the numerical integration. A very fine finite-element mesh could be used to solve this problem, but then the computational costs of the stress analysis may become prohibitive.

An arbitrary number of evaluation points can be generated, if the shape functions of the finite-elements is used to interpolate the stress field between the Gauss points of the finite-element mesh. Using these additional points conventional numerical integration methods can again be applied to calculate the volume integral eqn (12) or eqn (19). This procedure is implemented in the STAU computer code and its extensions (STAULE for lifetime evaluation and STAUB for proof testing)

4 Notches in Ceramic Components

4.1 Normalised stress integral H

The stress field of a notched tensile bar for various notch geometries was calculated using a linear eleastic finite-element analysis. Figure 1 shows the geometry of the bar with a typical finite-element mesh. The stress field in the notched cross-section is given in Fig. 2, which also illustrates the characteristics of the stress field, namely the stress-concentration factor:

$$\alpha_k = \frac{\sigma_{1,\,max}}{\sigma_{nom}} \tag{22}$$

and the normalised stress gradient

$$\chi^* = \frac{1}{\sigma_{1,\,max}} \cdot \left.\frac{d\sigma_1}{dx}\right|_{x=0} \tag{23}$$

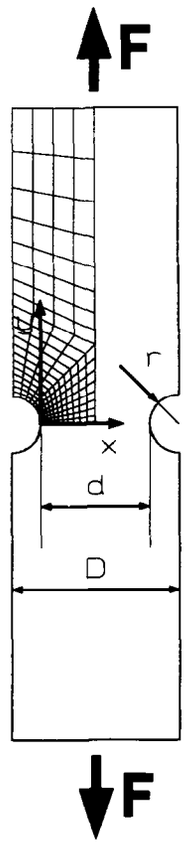

Fig. 1. Geometry of notched tensile bar with typical finite-element mesh.

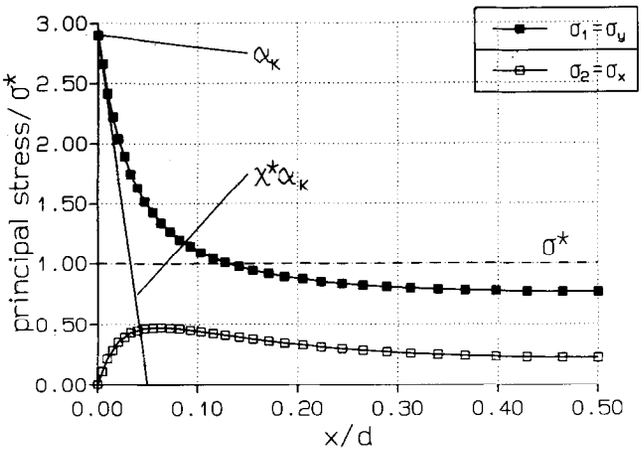

Fig. 2. Stress distribution in the notched cross-section.

where $\sigma_{1,max}$ is the maximum stress in the notch root ($x = 0$) and σ_{nom} is the nominal stress.

The geometries of the notches considered are shown in Fig. 3. The width of the notched cross-section d was kept constant in all cases. With these geometries a wide range of α_k–χ^*-values has been covered (see Table 1, $1{\cdot}9 < \alpha_k < 5$ and $0{\cdot}3 < \chi^* < 2$). The normalised stress gradient χ^* could be evaluated with sufficient accuracy only for those notches for which the notch roots were situated on the $y = 0$ symmetry line of the structure because of the limitations imposed by the finite-element mesh.

The normalised stress integral H, eqn (19), was calculated for these notched tensile bars using the finite-element code ABAQUS and the post-processor STAU.[10] The reference stress σ^* in eqn (19) was set equal to the nominal stress. The equivalent stress was determined using eqn (10).

All dimensions including the unit volume V_0 were given in mm. The thickness of the bars was assumed to be equal to 1, the nominal width d was 40, and the length L was 90.

Figure 4 shows the variation of the normalised stress integral H with the stress concentration factor α_k. For low values of the Weibull exponent m, the value of H depends only weakly on the stress concentration factor whereas H approaches α_k for

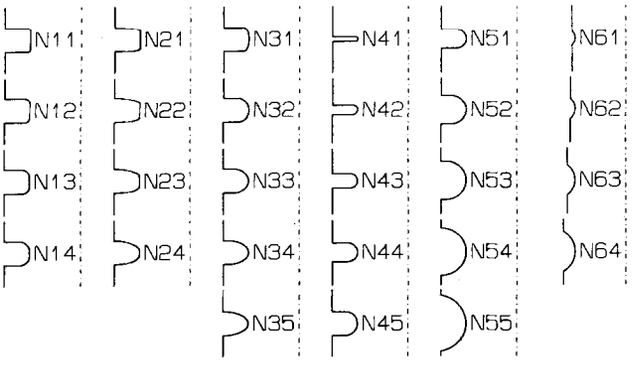

Fig. 3. Notch geometries.

Table 1. Dimension of notches defined in Fig. 3 in notched tensile bars with length L = 90 mm and nominal thickness d = 40 mm

Notch number	α_k, *eqn (22)*	χ^*, mm^{-1}, *eqn (23)*	$\frac{D}{d}$, *see Fig. 1*
N11	3·65	—	1·250
N12	2·99	—	1·250
N13	2·71	—	1·250
N14	2·55	—	1·250
N21	5·03	—	1·250
N22	4·05	—	1·250
N23	3·60	—	1·250
N24	3·32	—	1·250
N31	2·15	—	1·250
N32	2·48	—	1·250
N33	2·85	—	1·250
N34	3·17	—	1·250
N35	3·46	0·63	1·250
N41	4·97	1·21	1·250
N42	3·84	0·75	1·250
N43	3·27	0·50	1·250
N44	2·92	0·47	1·250
N45	2·67	0·38	1·250
N51	2·90	1·00	1·250
N52	2·47	0·70	1·250
N53	2·21	0·52	1·250
N54	2·04	0·42	1·250
N55	1·91	0·35	1·250
N61	1·95	1·19	1·030
N62	1·90	0·82	1·045
N63	1·92	0·57	1·075
N64	1·89	0·49	1·115

high values of m, i.e. low scatter of the materials' strength. In the deterministic limit ($m \to \infty$), only the maximum stress $\sigma_{1,max}$ contributes to the failure probability and H is equal to α_k. The influence of the shape of the notch is small compared to the influence of the stress-concentration factor for realistic values of m, as notches of very difficult shapes such as N21 and N41 yield H-values $H_{21} = 3{\cdot}53$ and $H_{41} = 3{\cdot}40$, respectively, for $m = 15$ which are

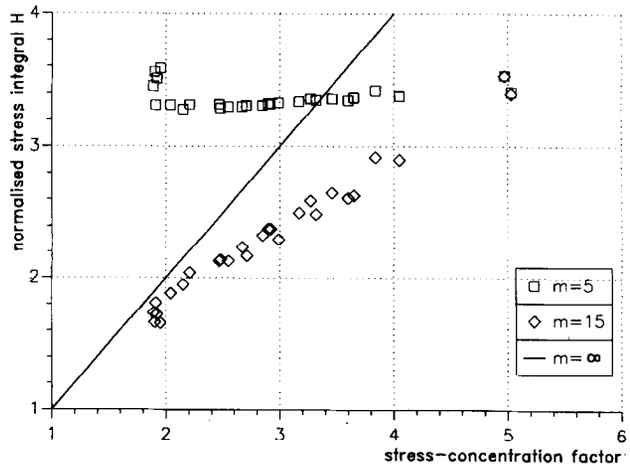

Fig. 4. Dependence of the normalised stress integral H on the stress concentration factor α_k; $m = \infty$ deterministic limit with $H = \alpha_k$.

much closer to each other than the values obtained from notches of similar shapes and different values of α_k (e.g. N11 and N21: $H_{11} = 2{\cdot}63$ and $H_{21} = 3{\cdot}40$).

Because of the strong correlation between α_k and χ^* for most of the examples studied here a special class of notches was selected with almost constant $\alpha_k = 1{\cdot}9$ and $0{\cdot}35 < \chi^* < 1{\cdot}2$ (N55, N61–64 in Fig. 3). These notches are compared to notches with $\alpha_k \propto \chi^*$ and χ^* in the same order of magnitude (N51–55 in Fig. 3). Figure 5(a, b) show the normalised stress integral H as a function of χ^* in both cases.

A reduced nominal thickness of $d = 20$ was used in this case in order to obtain more accurate values for the stress gradients. The effect of the nominal width on the normalised stress integral H is quite important, especially for low values of m, as can be seen by comparing Fig. 4 with Fig. 5(a).

The relationship between H and χ^* (Fig. 5(a)) looks very similar to that between H and α_k for N51–55 (Fig. 4), i.e. the effect of the stress gradient

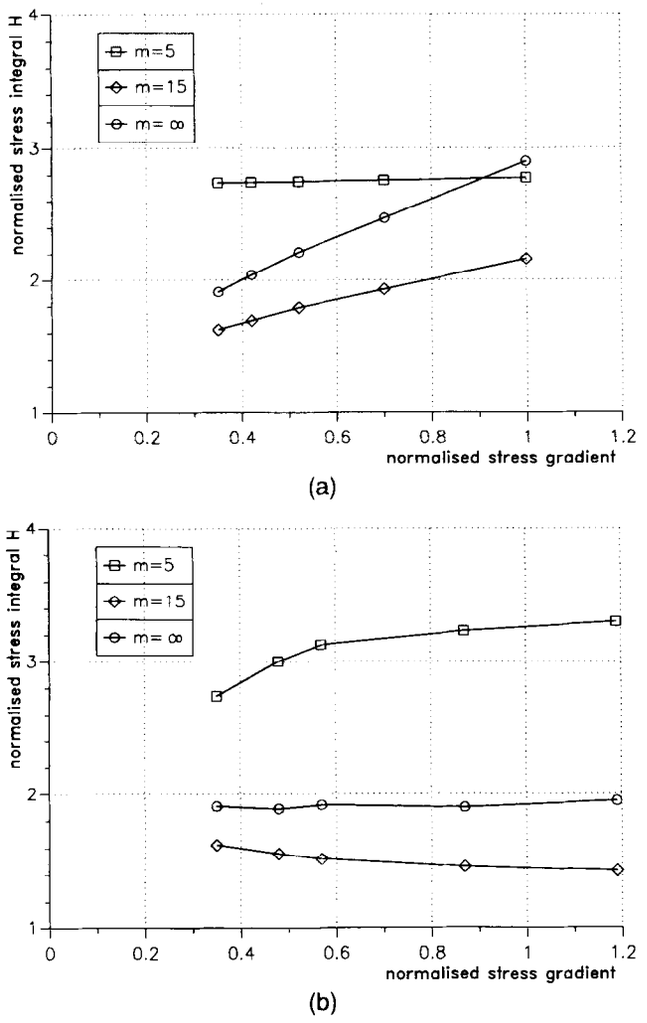

Fig. 5. (a) Dependence of the normalised stress integral H on the normalised stress gradient χ^*; notches with $\alpha_k \propto \chi^*$ (N51–55). (b) Dependence of the normalised stress integral H on the normalised stress gradient χ^*; notches with $\alpha_k \approx 1{\cdot}9$ (N55 and N61–64).

cannot be separated from the effect of the peak stress in the notch root. The increase in H with χ^* (i.e. a steeper gradient of the stress in the notch root) observed for $m = 5$ in the case of N55 and N61–64 (see Fig. 5(b)) is due to the fact that the stress gradient χ^* increases with increasing total width D (see Table 1). The nominal width and the nominal stress were kept constant, and hence a larger value of D implies that the stress in the remainder of the bar outside the notched cross-section decreases. H decreases with increasing χ^* for $m = 15$, because the width effect is suppressed and the change of the stressed volume in the notched cross-section becomes dominant.

4.2 Local risk of rupture for notches

The influences on the value or the normalised stress integral H can be clarified using the local risk of rupture as introduced in ref. 11. The following sub-volumes of the notched tensile bar are defined (see Fig. 6):

- V1 depending on the peak stress and on χ^* with

$$0 \le \rho \le r_\omega(\omega) = r_c \cdot (1 + \frac{4}{\pi}\omega), \qquad 0 \le \omega \le \frac{\pi}{2}$$

- V2 characterizing the distribution of the stress field in the centre of the notched cross-section with

$$r_\omega = r_c \cdot (1 + \frac{4}{\pi}\omega) < \rho \le \frac{d}{2} \qquad 0 \le \omega \le \frac{\pi}{2}$$

- V3 depending on the gradient of the stress field along the notch contour with

$$0 \le \rho \le 3r_c, \frac{\pi}{2} < \omega \le \frac{5\pi}{8}$$

- V4 linking V3 to the unnotched bar with

$$3r_c < \rho \le \frac{d}{2}, \quad \frac{\pi}{2} < \omega \le \frac{5\pi}{8}$$

- V5 taking care of the contribution from the remainder of the bar:

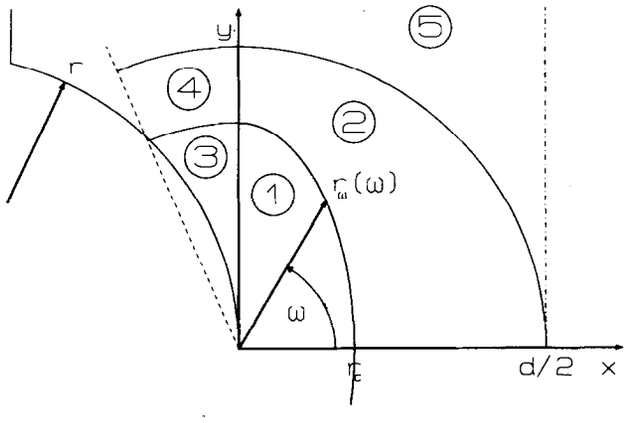

Fig. 6. Definition of the sub-volumes V1–5.

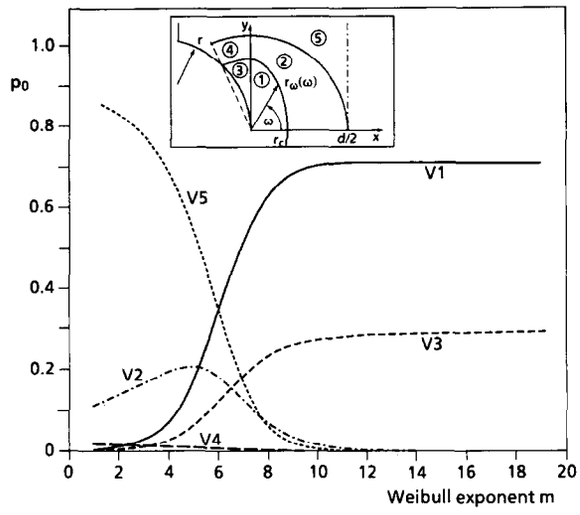

Fig. 7. Local risk of rupture p_0 for the sub-volumes V1–5; notch N51.

$$0 \le x \le \frac{d}{2} \text{ and } \frac{d}{2} < y \le \frac{L}{2};$$

$$0 \le x \le \frac{d}{2} \text{ and } \sqrt{x^2 + y^2} > \frac{d}{2}.$$

Here ρ denotes the distance from the notch root, ω the polar angle as shown in Fig. 6, and r_c is defined as

$$r_c = \frac{d}{2} \cdot \left(1 - \sqrt{1 - \frac{4(\alpha_k - 1)}{\alpha_k \cdot \chi^* \cdot d}}\right) \tag{24}$$

The local risk of rupture of sub-volume Vi is equal to:[9,11]

$$p_0(Vi) = \frac{\int_{Vi}\int_{\Omega} \sigma_{eq}{}^m \, d\Omega \, dV}{\int_{V}\int_{\Omega} \sigma_{eq}{}^m \, d\Omega \, dV} \tag{25}$$

$p_0(Vi)$ is equal to the probability that the worst flaw triggering fracture is contained in Vi. The local risk of rupture is depicted in Fig. 7 for notch N51. Similar pictures are obtained for other notch geometries. Figure 7 shows that the highest risk of rupture is associated with sub-volume V5 for low values of m. This implies that the stress field in the remainder of the notched tensile bar outside the notched cross-section dominates the failure probability. The notch geometry, on the other hand, influences the stress field in sub-volumes V1 and V3 which determine the failure probability for $m \ge 8$.

4.3 Approximation formula for H

The stress field of the notched tensile bars depends on the stress concentration factor α_k, the normalised stress gradient χ^*, and the relative notch depth d/D. Although the detailed stress distribution may be quite complicated (see e.g. ref. 1), a comparatively coarse approximation of the stress field may be sufficient in order to determine the normalised stress integral H, which depends mainly on α_k (m large) or on the stressed volume (m small).

The following relation is used for the maximum principal stress of a notched tensile bar:

$$\frac{\sigma_1}{\sigma^*} = \begin{cases} \alpha_k \cdot (1 - \chi^* \cdot r_c \cdot \dfrac{\rho}{r_\omega(\omega)}) \text{ in V1} \\ \alpha_k \cdot (1 - \chi^* \cdot r_c) \text{ in V2 and V4} \\ \alpha_k \cdot (1 - \chi^* \cdot \dfrac{\rho}{3}) \text{ in V3} \\ \dfrac{d}{D} \text{ in V5} \end{cases} \tag{26}$$

where V1–5 and $r_\omega(\omega)$ were defined in Section (2) and r_c follows from eqn (24). The approximate stress field, eqn (26), decreases linearly in the notched cross-section with the gradient—$\alpha_k \cdot \chi^*$ until it attains a constant value. It fulfils the equilibrium condition in the notched cross-section. The second principal stress is small compared to σ_1 in the vicinity of the notch root (see Fig. 2) and is set equal to zero.

The normalised stress integral H, eqn (19) can be split up into a volume integral and an integral over the orientation angles:

$$\begin{aligned} H &= H_v \cdot H_\Omega \\ H_v &= \frac{1}{V_0}\int_V \left(\frac{\sigma_1}{\sigma^*}\right)^m dV \\ H_\Omega &= \frac{1}{4\pi}\int_\Omega \left(\frac{\sigma_{eq}}{\sigma_1}\right)^m d\Omega. \end{aligned} \tag{27}$$

The following relations are obtained from eqn (26) for the contributions of the sub-volumes V1–5:

$$H^m_{V1} = \frac{13\pi}{6} \cdot \alpha_k{}^m \cdot \frac{1 - (1 - \chi^* r_c)^{m+1} \cdot (\chi^* r_c(m+1) + 1)}{(\chi^*)^2 \cdot (m+1) \cdot (m+2)} \tag{28}$$

$$H^m_{V2} = \frac{\pi}{12} \cdot \alpha_k{}^m \cdot (1 - \chi^* r_c)^m \cdot \left(\frac{3}{4}d^2 - 13r_c^2\right) \tag{29}$$

$$H^m_{V3} = \frac{9\pi}{8} \cdot \alpha_k{}^m \cdot \frac{1 - (1 - \chi^* r_c)^{m+1} \cdot (\chi^* r_c(m+1) + 1)}{(\chi^*)^2 \cdot (m+1) \cdot (m+2)} \tag{30}$$

$$H^m_{V4} = \frac{\pi}{16} \cdot \alpha_k{}^m \cdot (1 - \chi^* r_c)^m \cdot \left(\frac{1}{4}d^2 - 9r_c^2\right) \tag{31}$$

and

$$H^m_{V5} = \left(\frac{d}{D}\right)^m \cdot \frac{d^2}{4} \cdot \left(\left(\frac{L}{d} - 1\right) \cdot \frac{D}{d} + 1 - \frac{\pi}{4}\right). \tag{32}$$

The value of H_Ω eqn (27); can be determined by straightforward numerical integration, as the

equivalent stress σ_{eq} depends only on one polar angle for uniaxial stress states, (see eqns (4)–(8)). A closed-form analytical solution can be obtained in special cases (see Appendix). Combining eqns (28)–(32), the normalised stress integral follows from:

$$H = (4 \cdot (H_{V1}^{m} + H_{V2}^{m} + H_{V3}^{m} + H_{V4}^{m} + H_{V5}^{m})^{\frac{1}{m}} \cdot H_{\Omega}. \quad (33)$$

Figure 8 shows the H-values obtained from eqns (8)–(33) and the H-values obtained by numerical integration of the stress field which had been determined by a finite-element analysis. The agreement obtained for notches N51 and N55 is very good.

It should be kept in mind, however, that eqns (27)–(33) are applicable only in cases where the notch root lies on the symmetry line. There are greater deviations for non-central notches as can be concluded from Fig. 4 which shows the variation of H for a given value of α_k. It may also be difficult in these cases to obtain reliable values of χ^*. In all cases considered in this paper the following relationships hold for $m > 10$

$$H \propto \frac{\alpha_k^m}{\chi^{*2} \cdot m^2} \quad (34)$$

and, according to eqn (A12):

$$H_{\Omega}^{m} \propto \frac{1}{m} \quad (35)$$

with an accuracy of about 10%. Combining eqns (34) and (35) leads to the following expression for the stress integral H:

$$H \propto \frac{\alpha_k}{(\chi^{*2} \cdot m^3)^{\frac{1}{m}}}. \quad (36)$$

In using this relation it should be kept in mind that it was derived on the basis of a limited number of examples and is strictly speaking only applicable to cases with very similar notch contours in a uniaxial stress field. However, additional examples not included in this paper showed a very similar behaviour. Hence it is felt that the relation (36) can be used in a somewhat more general sense, and that it yields the dependence of the leading term of the failure probability on characteristic quantities such as the stress concentration factor, the normalised stress gradient, and the Weibull modulus.

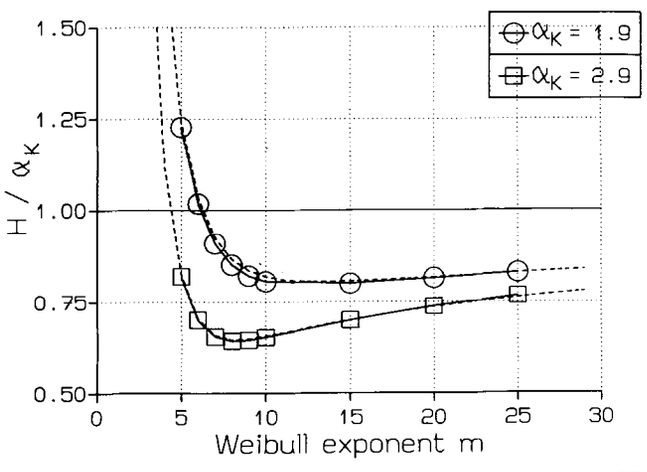

Fig. 8. Comparison of the analytical approximation for H, eqns (28)–(33), with the results of the finite-element analysis; - - - analytical solution; — numerical analysis.

5 Conclusion

The influence of notches on the reliability of ceramic components can be assessed using a normalised stress integral. The stress-concentration factor α_k in the notch root is the most important influencing factor which implies that notches of different shapes but similar values of α_k yield similar values of the stress integral. This conclusion was drawn from results obtained with tensile bars containing circular notches. The local risk of rupture in the vicinity of the notch root approaches unity for $m > 8$, i.e. failure is almost always caused by flaw located near the notch root. This is why a linear approximation of the stress field in the vicinity of the notch root, from which a closed-form solution of the stress integral can be derived, agrees very well with the values of the stress integral obtained by numerical integration of the exact stress field.

References

1. Neuber, H., *Kerbspannungslehre*, Springer Publ., Berlin, 1989.
2. Peterson, R. E., *Stress Concentration Factors*, J. Wiley Publ., New York, 1974.
3. Batdorf, S. B. & Crose, J. G., A statistical theory for the fracture of brittle structures subjected to nonuniform stress. *J. Appl. Mechanics*, **41** (1974) 459–61.
4. Batdorf S. B. & Heinisch, H. L., Weakest link theory reformulated for arbitrary fracture criterion. *J. Am. Ceram. Soc.*, **61** (1978) 355–8.
5. Evans A. G., A general approach for the statistical analysis of multiaxial fracture. *J. Am. Ceram. Soc.*, **61** (1978) 302–8.
6. Matsuo Y., A probabilistic analysis of fracture loci under bi-axial stress state. *Bull. JSME*, **24** (1981) 290–4.
7. Thiemeier, T., Brückner-Foit, A. & Kölker, H., Influence of the fracture criterion on the failure probability of ceramic components. *J. Am. Ceram. Soc.*, **74** (1991) 48–52.
8. Paris P. C. & Sih, G. C., Stress Analysis of Cracks. In *Fracture Toughness Testing and its Applications*, ASTM STP 381, American Society of Testing of Materials, Philadephia, PA, 1965, pp. 30–83.
9. Matsuo, Y. & Kitakami, K., On the statistical theory of fracture location combined with competing risk theory. In *Fracture Mechanics of Ceramics*, Vol. 7, eds, R. C. Bradt *et al.*, Plenum Press, New York, 1986, pp. 223–35.

10. Heger, A., Brückner-Foit, A. & Munz D., STAU — ein Programm zur Berechnung der Ausfallwahrscheinlichkeit mehrachsig beanspruchter keramischer Komponenten als Post-Prozessor für Finite-Elemente-Programme. Internal Report, Institute for Reliability and Failure Analysis, University of Karlsruhe, Germany, 1991.
11. Brückner-Foit A., Heger, A. & Munz D., Effect of proof testing on the failure probability of multiaxially loaded ceramic components. *ASTM STP 1202*, American Society for Testing and Materials Philadelphia, PA, 1993, pp. 346–59.

Appendix

A uniaxial stress state leads to the following relations for the normal stress σ_n (mode I loading) and the shear stress τ (mode II loading):

$$\sigma_n = \sigma_1^2 \cdot \cos^2\theta \tag{A1}$$

$$\tau = \sigma_1 \cdot |\sin\theta \cos\theta| \tag{A2}$$

where eqns (4)–(7) have been used. Equation (10) yields for the equivalent stress:

$$\sigma_{eq} = \sigma_1 \cdot |\cos\theta| \cdot \sqrt{\cos^2\theta + \left(\frac{2}{2-\nu}\right)^2 \sin^2\theta}\,. \tag{A3}$$

Hence the integral H_Ω, eqn (27), has the following form:

$$H\Omega^m = \int_0^{\frac{\pi}{2}} \left(\cos^2\theta + \left(\frac{2}{2-\nu}\right)^2 \sin^2\theta\right)^{\frac{m}{2}} \cdot \cos^m\theta \cdot \sin\theta \, d\theta \tag{A4}$$

which can be integrated in closed form for even values of m.

With the binomial relation

$$\left(\cos^2\theta + \left(\frac{2}{2-\nu}\right)^2 \sin^2\theta\right)^{\frac{m}{2}} = \sum_{k=0}^{m/2} \binom{m/2}{k} \cdot \left(\frac{2}{2-\nu}\right)^{2k} \cdot \sin^{2k}\theta \cdot \cos^{m-2k}\theta \tag{A5}$$

and the substitution $x = \cos\theta$, the integral eqn (A4) can be written as:

$$H\Omega^m = \sum_{k=0}^{m/2} \int_0^1 \binom{m/2}{k} \cdot \left(\frac{2}{2-\nu}\right)^{2k} x^{2m-2k} \cdot (1-x^2)^k \, dx \tag{A6}$$

The following relation can be derived by successive integration by parts:

$$\int_0^1 x^{2m-2k} \cdot (1-x^2)^k \, dx = \frac{k! \cdot 2^k}{(2m+1) \cdot (2m-1) \cdot \ldots \cdot (2m-2k+1)} \tag{A7}$$

which leads to the following expression for Hω:

$$H\Omega^m = \frac{1}{2m+1} \sum_{k=0}^{m/2} \left(\frac{2}{2-\nu}\right)^{2k} \cdot \frac{m \cdot (m-2) \cdot \ldots \cdot (m-2k+2)}{(2m-1) \cdot (2m-3) \cdot \ldots \cdot (2m-2k+1)} \tag{A8}$$

Equation (A8) is valid only for even values of m. The orientation integral Hω for general values of m can be obtained by interpolation.

Equation (A8) can be simplified using

$$\frac{m-2l}{2m-2l-1} \le \frac{m-2l}{2m-4l} = \frac{1}{2} \text{ for } l = 1, \ldots, \frac{m}{2} - 1 \tag{A9}$$

and

$$\frac{m-2l}{2m-2l-1} \ge \frac{m-2l}{2m-1} \ge \frac{2}{2m-1} \text{ for } l = 0, \ldots, \frac{m}{2} - 1. \tag{A10}$$

The following bounds are obtained for $H\Omega$ after some re-arrangement of the sums:

$$\frac{1}{2m+1} \cdot \frac{1 - \left(\left(\frac{2}{2-\nu}\right)^2 \cdot \frac{2}{2m-1}\right)^{\frac{m}{2}+1}}{1 - \left(\frac{2}{2-\nu}\right)^2 \cdot \frac{2}{2m-1}} \le H\Omega^m \tag{A11}$$

$$\le \frac{1}{2m+1} \cdot \frac{1 - \left(\left(\frac{2}{2-\nu}\right)^2 \cdot \frac{1}{2}\right)^{\frac{m}{2}+1}}{1 - \left(\frac{2}{2-\nu}\right)^2 \cdot \frac{1}{2}} - \frac{1}{(2m+1)(2m-1)}$$

These bounds can be used to obtain an estimate of $H\Omega$ for general values of m, since $H\Omega$ is a smooth function of m. Equation (A11) implies that

$$H\Omega^m \propto \frac{1}{m} \tag{A12}$$

for $m \ge 10$. The same relationship can be obtained for other criteria with the proportionality factor depending on the multiaxiality criterion.